Diagrammatic approach for open chaotic systems

Oded Agam
The Racah Institute of Physics, The Hebrew University, Jerusalem 91904, Israel
(Received 24 June 1999)

A semiclassical diagrammatic approach is constructed for calculating correlation functions of observables in open chaotic systems with time reversal symmetry. The results are expressed in terms of classical correlation functions involving Wigner representations of the observables. The formalism is used to explain a recent microwave experiment on the four-disk problem, and to characterize the two-point function of the photodissociation cross section of complex molecules.

PACS number(s): 05.45.−a, 03.65.Sq, 24.60.−k

I. INTRODUCTION

An experimental enquiry of the internal structure of a complex system involves, usually, some type of a scattering process. For instance, a photon is scattered from the system and then collected by a remote detector. In other situations, the collected objects are fragments of the initial system itself. A prototype example of the latter process is the photodissociation of molecules: The molecule absorbs a photon, and disintegrates by redistribution of energy in its vibrational modes [1]. A common feature of such systems is the coupling to continuum modes. That is, above some energy threshold, the system is open.

Open systems are characterized by resonances. These are eigenstates of open Hamiltonians which are normalizable, and therefore correspond to complex eigenvalues associated with a decay in time. In the most interesting situations, this decay is sufficiently slow, allowing for the system to explore a large part of the phase space before disintegration. In complex systems, such as nuclei or large molecules, the dynamics on these long lived resonances is chaotic; therefore, the expectation value of a generic observable exhibits a statistical behavior [2]. For instance, the absorption cross section for photodissociation of large molecules is a pseudorandom function of the photon energy [3–5]. This behavior suggests a statistical analysis of observables in open chaotic systems [6–12].

The main purpose of this paper is to construct a diagrammatic scheme for calculating correlators of observables in open chaotic systems. This diagrammatic approach is similar to the cross diagram technique in disordered systems [13]. However, although both techniques rely on the semiclassical approximation, there are differences: The main advantage of the proposed scheme is in its capability of describing individual systems rather than an ensemble of them. Ensemble averaging, as opposed to the energy averaging employed here, tends to erase ''clean'' features of individual systems. These features may have important manifestations, as will be demonstrated in this paper. On the other hand, disorder diagrammatics provides a systematic way of calculating corrections due to quantum interference effects. At this stage we are not able to provide a similar prescription for general chaotic systems. Therefore, we confine our attention to open systems with decay time shorter than the time at which weak localization effects set in. The latter time scale, known as the Ehernfest time, diverges logarithmically in the semiclassical limit [14].

The semiclassical analysis of a quantum system brings out the relation to its underlying classical dynamics [15]. For example, the classical dynamics of an electron in a disordered metal is diffusive, and ensemble averages of quantum observables of the electron are expressed in terms of the spectral properties of the diffusion propagator [16]. In more general situations the classical evolution is described by the Perron-Frobenius operator whose spectrum, known as the Ruelle resonances [17,18], describes the irreversible relaxation of probability densities in phase space.

The classical spectrum of the system sets the important time scales of the problem. When the system is almost close there are two significant time scales: One is the decay time of the system, τ_d, which is inversely proportional to the typical width of the resonances. The closer the system, the longer the decay time. The second time scale τ_c is the time it takes for a classical density distribution to relax to the ergodic state on the energy shell, when the system is closed. In diffusive systems this time is known as the Thouless time [19].

A large separation between the classical time scales, $\tau_d \gg \tau_c$, implies a universal statistical behavior of the system on energy scales smaller than $\hbar/\tau_c$. That is, the statistics is described by a random matrix theory [20] suitable for open systems [21,22]. However, as will be demonstrated in this paper, there are important manifestations of the nonuniversal behavior of the system, which are especially pronounced when τ_d is of the same order as τ_c. The main use of the diagrammatic approach will be to calculate these individual imprints of the system. This information is most important for constructing effective models from experimental data.

The organization of this paper is as follows. In Sec. II we derive the classical propagator of the system by an energy averaging of the Green functions. This propagator constitutes the basic building block of the diagrammatic approach developed in Sec. III. We shall restrict our considerations to systems with time reversal symmetry. In Sec. IV we present two applications of the formalism. One concerns the microwave experiment on the N-disk scattering system [23]. The second is the photodissociation absorption cross section of complex molecules. In Sec. V we summarize our results, and mention directions of further studies.

II. CLASSICAL PROPAGATION FROM QUANTUM GREEN FUNCTIONS

The purpose of this section is to construct the building blocks of the diagrammatic scheme which will be developed in this paper. It is the classical propagator, which is a generalization of the ''diffuson'' ladder diagrams of disordered systems [13]. Our construction will rely on the semiclassical approximation for the Green function of the quantum system [24,25].

A. Semiclassical Green function

Let $\hat{\mathcal{H}}$ be the Hamiltonian of an open system having d degrees of freedom, and $\mathcal{H}(\mathbf{x})$ be its classical counterpart, where $\mathbf{x}=(\mathbf{r},\mathbf{p})$ is a point in the classical phase space. The advanced ($^+$) and retarded ($^-$) Green functions of the system are

$$G^{\pm}(\epsilon)=\frac{1}{\epsilon\pm i0-\hat{\mathcal{H}}},$$

where $i0$ denote an infinitesimal positive imaginary part. In the semiclassical limit, these Green functions contain two contributions:

$$G^{\pm}\simeq G_W^{\pm}+G_{osc}^{\pm}.$$

The first, known as the Weyl term, is a smooth function of the energy given by

$$\langle \mathbf{r}'|G_W^{\pm}(\epsilon)|\mathbf{r}\rangle=\int\frac{d\mathbf{p}}{h^d}\frac{e^{(i/\hbar)\mathbf{p}\cdot(\mathbf{r}'-\mathbf{r})}}{\epsilon\pm i0-\mathcal{H}(\mathbf{x})}, \tag{1}$$

where $h=2\pi\hbar$ is Planck's constant, and $\mathbf{x}=((\mathbf{r}+\mathbf{r}')/2,\mathbf{p})$. The second contribution is an oscillatory function of the energy expressed as a sum over the classical trajectories [24] from $\mathbf{r}$ to $\mathbf{r}'$ with energy ϵ:

$$\langle \mathbf{r}'|G_{osc}^{+}(\epsilon)|\mathbf{r}\rangle=\sum_{\mu}A_{\mu}e^{(i/\hbar)S_{\mu}(\mathbf{r}',\mathbf{r};\epsilon)},$$
$$\langle \mathbf{r}|G_{osc}^{-}(\epsilon)|\mathbf{r}'\rangle=\sum_{\mu}A_{\mu}^{*}e^{-(i/\hbar)S_{\mu}(\mathbf{r}',\mathbf{r};\epsilon)}. \tag{2}$$

Here $S_{\mu}(\mathbf{r}',\mathbf{r};\epsilon)$ is the classical action of the μth trajectory, while A_{μ} is an amplitude which can be expressed as a combination of second derivatives of $S_{\mu}(\mathbf{r}',\mathbf{r};\epsilon)$ with respect to $\mathbf{r}'$ and $\mathbf{r}$.

B. Classical propagator

To construct the classical propagator of the system from an energy average of Green functions, consider the function

$$\Pi(\mathbf{x}',\mathbf{x};\omega)=\langle \mathrm{Tr}\{G^{+}(\epsilon+\hbar\omega)\delta(\hat{\mathbf{x}}-\mathbf{x})G^{-}(\epsilon)\delta(\hat{\mathbf{x}}-\mathbf{x}')\}\rangle, \tag{3}$$

where the δ-function operator is defined by the symmetric Fourier transform [26]

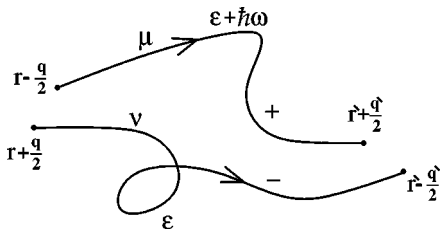

FIG. 1. An illustration of the classical trajectories contributing to the advanced (+) and the retarded (−) Green functions in Eq. (5) before the energy averaging.

$$\delta(\hat{\mathbf{x}}-\mathbf{x})=\int\frac{d\mathbf{q}d\mathbf{k}}{h^{2d}}e^{(i/\hbar)[\mathbf{k}\cdot(\hat{\mathbf{r}}-\mathbf{r})+\mathbf{q}\cdot(\hat{\mathbf{p}}-\mathbf{p})]}. \tag{4}$$

Although not written explicitly, it will be assumed that these δ functions have a small finite width, say the integration over $\mathbf{k}$ and $\mathbf{q}$ is limited to a large hypersphere. This width will be taken to zero at the end of the calculation. Substituting definition (4) in Eq. (3), we obtain

$$\Pi(\mathbf{x}',\mathbf{x};\omega)=\int\frac{d\mathbf{q}d\mathbf{q}'}{h^{2d}}e^{-(i/\hbar)(\mathbf{p}\cdot\mathbf{q}+\mathbf{p}'\cdot\mathbf{q}')}\times\left\langle G^{+}\left(\mathbf{r}'+\frac{\mathbf{q}'}{2},\mathbf{r}-\frac{\mathbf{q}}{2};\epsilon+\hbar\omega\right)\times G^{-}\left(\mathbf{r}+\frac{\mathbf{q}}{2},\mathbf{r}'-\frac{\mathbf{q}'}{2};\epsilon\right)\right\rangle. \tag{5}$$

Next we substitute the semiclassical approximation for the Green functions. Each Green function has a smooth and an oscillatory contribution; thus there are four terms in $\Pi(\mathbf{x}',\mathbf{x};\omega)$. However, it is easy to see that two of them, $\langle G_W^{\pm}G_{osc}^{\mp}\rangle$, vanish upon averaging. Therefore only the Weyl contribution, $\langle G_W^{+}G_W^{-}\rangle$, and the oscillatory contributions $\langle G_{osc}^{+}G_{osc}^{-}\rangle$, survive.

The Weyl term is local in phase space, that is it is significant only when $\mathbf{x}\simeq\mathbf{x}'$. This term, which we denote by $\Pi_{loc}(\mathbf{x}',\mathbf{x};\omega)$, is of minor importance for our purposes, and we defer its calculation to Appendix A. The result, however, is

$$\Pi_{loc}(\mathbf{x}',\mathbf{x};\omega)=\frac{2\pi}{-i\hbar h^{d}\omega^{+}}\delta(\mathbf{x}'-\mathbf{x})\delta(\epsilon-\mathcal{H}(\mathbf{x})), \tag{6}$$

where $\omega^{+}=\omega+i0$.

Consider now the contribution from the oscillatory parts of the Green functions. The product $G_{osc}^{+}G_{osc}^{-}$ consists of a double sum over trajectories: μ from $\mathbf{r}-\mathbf{q}/2$ to $\mathbf{r}'+\mathbf{q}'/2$ and ν from $\mathbf{r}+\mathbf{q}/2$ to $\mathbf{r}'-\mathbf{q}'/2$; thus

$$G_{osc}^{+}(\epsilon+\hbar\omega)G_{osc}^{-}(\epsilon)\simeq\sum_{\mu\nu}A_{\mu}A_{\nu}^{*}e^{iS_{\mu}-iS_{\nu}}. \tag{7}$$

An illustration of two such orbits is depicted in Fig. 1. This term is, clearly, nonlocal in space. Its oscillatory dependence on the energy implies that upon energy averaging the main contribution comes from the diagonal part ($\mu=\nu$) of the double sum (7). The approximation of a double sum by a

single sum is called the ''diagonal approximation'' [27]. It does not take into account quantum interference corrections such as weak localization. However, according to our assumptions on the relation between the Ehernfest time and the decay time of the system, these corrections can be neglected.

The construction of the diagonal sum of orbits involves an expansion of the actions around that of the orbit going from $\mathbf{r}$ to $\mathbf{r}'$, namely,

$$S_\mu\left(\mathbf{r}'+\frac{\mathbf{q}'}{2},\mathbf{r}-\frac{\mathbf{q}}{2};\epsilon+\hbar\omega\right)\simeq S_\mu(\mathbf{r}',\mathbf{r};\epsilon)\hbar\omega t_\mu + \frac{1}{2}(\mathbf{p}_\mu\cdot\mathbf{q}+\mathbf{p}'_\mu\cdot\mathbf{q}'),$$

$$S_\nu\left(\mathbf{r}'-\frac{\mathbf{q}'}{2},\mathbf{r}+\frac{\mathbf{q}}{2};\epsilon\right)\simeq S_\nu(\mathbf{r}',\mathbf{r};\epsilon)-\frac{1}{2}(\mathbf{p}_\nu\cdot\mathbf{q}+\mathbf{p}'_\nu\cdot\mathbf{q}'),$$

where $\mathbf{p}_\mu$ and $\mathbf{p}'_\mu$ denote the initial (at point $\mathbf{r}$) and final (at point $\mathbf{r}'$) momenta associated with the μth orbit. Similarly $\mathbf{p}_\nu$ and $\mathbf{p}'_\nu$ are the initial and final momenta associated with the νth orbit. t_μ is the time which takes for the particle to travel along the μth trajectory. Using the above expansions for the actions in Eq. (7), the diagonal approximation yields

$$\langle G^-_{osc}(\epsilon+\hbar\omega)G^+_{osc}(\epsilon)\rangle=\sum_\mu |A_\mu|^2 e^{(i/\hbar)(\mathbf{p}_\mu\cdot\mathbf{q}+\mathbf{p}'_\mu\cdot\mathbf{q}'+\hbar\omega t_\mu)}.$$

Substituting this result into Eq. (5) and integrating over $\mathbf{q}$ and $\mathbf{q}'$ we arrive at

$$\Pi(\mathbf{x}',\mathbf{x};\omega)=\sum_{\text{orbits: } \mathbf{r}\to\mathbf{r}'} |A_\mu|^2 e^{i\omega t_\mu}\delta(\mathbf{p}-\mathbf{p}_\mu)\,\delta(\mathbf{p}'-\mathbf{p}'_\mu). \tag{8}$$

This formula expresses $\Pi(\mathbf{x}',\mathbf{x};\omega)$ as a sum over the classical trajectories from $\mathbf{r}$ to $\mathbf{r}'$. The momenta δ functions restrict the initial and final momenta of the trajectories to $\mathbf{p}$ and $\mathbf{p}'$, respectively.

The diagonal sum (8) can be calculated using the flowing sum rule [28] (proved in Appendix B):

$$h^{d-1}\hbar^2\sum_{\text{orbits: } \mathbf{r}\to\mathbf{r}'} |A_\mu|^2 g(\mathbf{x}'_\mu,\mathbf{x}_\mu,t_\mu) = \int_0^\infty dt\,d\mathbf{p}'\,d\mathbf{p}\,g(\mathbf{x}',\mathbf{x},t)\,\delta(\epsilon-\mathcal{H}(\mathbf{x}))\,\delta(\mathbf{x}'-\mathbf{x}(t)). \tag{9}$$

Here $g(\mathbf{x}',\mathbf{x},t)$ is a general function of the space points $\mathbf{x}'$ and $\mathbf{x}$, and the time t. The coordinates $\mathbf{x}_\mu=(\mathbf{r},\mathbf{p}_\mu)$ and $\mathbf{x}'_\mu=(\mathbf{r}',\mathbf{p}'_\mu)$ are the initial and final phase space points of the μth trajectory, while t_μ is the corresponding period of the trajectory. Finally, $\mathbf{x}(t)$ is the phase space trajectory of the system, as function of the time t, starting from $\mathbf{x}$. This trajectory is the solution of Hamilton's equations: $\dot{\mathbf{r}}=\partial\mathcal{H}(\mathbf{x})/\partial\mathbf{p}$ and $\dot{\mathbf{p}}=-\partial\mathcal{H}(\mathbf{x})/\partial\mathbf{r}$, with initial conditions $\mathbf{x}(t=0)=\mathbf{x}$. Using Eq. (9) to replace the sum over orbits in Eq. (8) by an integral over the time we finally obtain

$$\Pi(\mathbf{x}',\mathbf{x};\omega)=\delta(\epsilon-\mathcal{H}(\mathbf{x}))\int_0^\infty \frac{dt\;\; e^{i\omega t}}{h^{d-1}\hbar^2}\,\delta(\mathbf{x}'-\mathbf{x}(t)). \tag{10}$$

The function $\Pi(\mathbf{x}',\mathbf{x};\omega)$ is the Fourier transform of the classical propagator of the system for $t>0$. It is the generalization of the ''diffuson'' of disordered systems to general chaotic systems. This analogy becomes clearer when projecting $\Pi(\mathbf{x}',\mathbf{x};\omega)$ down to real space, i.e., integrating over $\mathbf{p}$ and $\mathbf{p}'$. The integration over $\mathbf{p}'$ is straightforward, and to integrate over $\mathbf{p}$ we assume that $\mathcal{H}(\mathbf{x})=p^2/2m$, and that $\mathbf{r}(t)$ is independent of $\mathbf{p}$. This is good approximation for a diffusive motion on long time scales, since momentum relaxation is fast. Thus

$$\int d\mathbf{p}'d\mathbf{p}\Pi(\mathbf{x}',\mathbf{x};\omega)\simeq\frac{2\pi\overline{\nu}}{\hbar}\int dt e^{i\omega t}\delta(\mathbf{r}'-\mathbf{r}(t)),$$

where $\overline{\nu}$ is the average density of states per unit volume. The function $\delta(\mathbf{r}'-\mathbf{r}(t))$, is the matrix element of the diffusion propagator between the position states $|\mathbf{r}\rangle$ and $\langle\mathbf{r}'|$, i.e.,

$$\delta(\mathbf{r}'-\mathbf{r}(t))=\langle\mathbf{r}'|e^{D\nabla^2 t}|\mathbf{r}\rangle,$$

where D is the diffusion constant. Inserting a complete set of momentum states, which diagonalizes the propagator, and integrating over t, we arrive at the formula for the diffuson of disordered systems:

$$\int d\mathbf{p}'d\mathbf{p}\Pi(\mathbf{x}',\mathbf{x};\omega)\simeq\frac{2\pi\overline{\nu}}{V\hbar}\sum_q\frac{e^{i\mathbf{q}\cdot(\mathbf{r}'-\mathbf{r})}}{-i\omega+Dq^2}, \tag{11}$$

where V is the volume of the system.

A spectral decomposition similar to Eq. (11) also exists for the classical propagator of general chaotic systems [17,18]. In the time domain one formally has

$$\delta(\mathbf{x}'-\mathbf{x}(t))=\langle\mathbf{x}'|e^{-\mathcal{L}t}|\mathbf{x}\rangle = \delta(\mathcal{H}(\mathbf{x})-\mathcal{H}(\mathbf{x}'))\sum_\alpha e^{-\gamma_\alpha t}\chi^l_\alpha(\mathbf{x})\chi^r_\alpha(\mathbf{x}'), \tag{12}$$

where $\mathcal{L}=\{\;\cdot\;,\mathcal{H}(\mathbf{x})\}$ is the Poisson bracket operator of the classical system, γ_α are its eigenvalues, and $\chi^l_\alpha(\mathbf{x})$ and $\chi^r_\alpha(\mathbf{x}')$ are the corresponding left and right eigenfunctions. The above spectral decomposition results from regularization of the classical dynamics. For instance, by keeping a finite width for the δ functions in Eq. (10), and taking it to zero only after the diagonalization of the propagator. The resulting eigenvalues, called Ruelle resonances, constitute the Perron-Frobenius spectrum of the classical system. All classical eigenvalues of open systems have positive real part. They appear either as purely real or in complex conjugate pairs, We denote this set of eigenvalues by $\{\gamma_\alpha\}_{\alpha=0}^\infty$, and order them according to the magnitude of their real parts, $\gamma'_0\leqslant\gamma'_1\leqslant\gamma'_2\leqslant\cdots$, where $\gamma_\alpha=\gamma'_\alpha\pm i\gamma''_\alpha$.

In concluding this section we remark that complex eigenvalues of the classical propagator, $\gamma_\alpha=\gamma'_\alpha\pm i\gamma''_\alpha$, characterize ballistic chaotic systems. They emerge, for example, when typical classical trajectories spend a long time near

some short periodic orbit. This type of behavior does not appear in diffusive systems where classical relaxation is dominated by purely real eigenvalues. In Sec. IV we demonstrate the manifestations of complex Ruelle resonances in two examples.

III. SEMICLASSICAL DIAGRAMMATICS FOR OPEN CHAOTIC SYSTEMS

In this section we construct a diagrammatic scheme for calculating correlation functions such as the two-point function $\langle \mathrm{Tr}\{G^+(\epsilon+\hbar\omega)\hat{A}\}\mathrm{Tr}\{G^-(\epsilon)\hat{B}\}\rangle$, where $\hat{A}$ and $\hat{B}$ are some observables, and the averaging $\langle\cdots\rangle$ is over the ''center of mass'' energy ϵ. The energy interval over which this averaging takes place is sufficiently wide to contain a large number of resonances, but narrow enough so that the classical dynamics within this interval is approximately independent of the energy.

The proposed diagrammatic scheme is a lift into phase space of the disordered diagrammatics which is embedded either in the momentum or real space. An important step in this direction is to express products of quantum observables in terms of their Wigner representations which are functions of phase space variables. This issue will be considered in Sec. III A. Next we calculate the one-point function (Sec. III B) , and the two-point function (Sec. III C) functions. Finally (Sec. III D), the results will be generalized to n-point functions by setting the diagram rules for their calculation.

A. Wigner representations

Let $\langle \mathbf{r}|\hat{A}|\mathbf{r}'\rangle$ be a matrix element of the observable $\hat{A}$, where $\langle\mathbf{r}|$ and $|\mathbf{r}'\rangle$ are position states in Dirac notation. The Wigner representation [29]

$$A(\mathbf{x})=\int d\mathbf{q}e^{(i/\hbar)\mathbf{p}\cdot\mathbf{q}}\left\langle \mathbf{r}-\frac{\mathbf{q}}{2}|\hat{A}|\mathbf{r}+\frac{\mathbf{q}}{2}\right\rangle \tag{13}$$

of the operator $\hat{A}$ is a function of the phase space variables $\mathbf{x}=(\mathbf{r},\mathbf{p})$. It is a faithful representation of the quantum operator, since all its matrix elements can be reconstructed from the inverse relation

$$\langle \mathbf{r}|\hat{A}|\mathbf{r}'\rangle=\int \frac{d\mathbf{p}}{h^d}e^{-(i/\hbar)\mathbf{p}\cdot(\mathbf{r}'-\mathbf{r})}A(\mathbf{x}), \tag{14}$$

where $\mathbf{x}=((\mathbf{r}'+\mathbf{r})/2,\mathbf{p})$. Expressed as a function on the classical phase space, the Wigner representation is convenient for semiclassical expansions.

The external product of two operators, $\hat{A}\otimes\hat{B}$, with matrix elements $\langle \mathbf{r}_0|\hat{A}|\mathbf{r}_1\rangle\langle \mathbf{r}_2|\hat{B}|\mathbf{r}_3\rangle$, has more than one Wigner representation. These representations correspond to the various ways by which pairs of coordinates are used for the Fourier transforms. One possibility is to pair the coordinates of each one of the operators separately, i.e., $\mathbf{r}_0$ with $\mathbf{r}_1$ and $\mathbf{r}_2$ with $\mathbf{r}_3$. Obviously, the result in this case will be the product of the Wigner representations of $\hat{A}$ and $\hat{B}$. Denoting this by $[AB]_d(\mathbf{x},\mathbf{x}')$, we have

$$[AB]_d(\mathbf{x},\mathbf{x}')=A(\mathbf{x})B(\mathbf{x}')=\int d\mathbf{q}d\mathbf{q}'e^{(i/\hbar)(\mathbf{p}\cdot\mathbf{q}+\mathbf{p}'\cdot\mathbf{q}')}\times\left\langle \mathbf{r}-\frac{\mathbf{q}}{2}|\hat{A}|\mathbf{r}+\frac{\mathbf{q}}{2}\right\rangle\left\langle \mathbf{r}'-\frac{\mathbf{q}'}{2}|\hat{B}|\mathbf{r}'+\frac{\mathbf{q}'}{2}\right\rangle, \tag{15}$$

where $\mathbf{x}=(\mathbf{r},\mathbf{p})$, and $\mathbf{x}'=(\mathbf{r}',\mathbf{p}')$. The two other representations correspond to different pairing configurations: $\mathbf{r}_0$ with $\mathbf{r}_3$ and $\mathbf{r}_1$ with $\mathbf{r}_2$, which leads to

$$[AB]_s(\mathbf{x},\mathbf{x}')=\int d\mathbf{q}d\mathbf{q}'e^{(i/\hbar)(\mathbf{p}\cdot\mathbf{q}+\mathbf{p}'\cdot\mathbf{q}')}\left\langle \mathbf{r}-\frac{\mathbf{q}}{2}|\hat{A}|\mathbf{r}'+\frac{\mathbf{q}'}{2}\right\rangle\times\left\langle \mathbf{r}'-\frac{\mathbf{q}'}{2}|\hat{B}|\mathbf{r}+\frac{\mathbf{q}}{2}\right\rangle, \tag{16}$$

and $\mathbf{r}_0$ with $\mathbf{r}_2$ and $\mathbf{r}_1$ with $\mathbf{r}_3$, which gives

$$[AB]_c(\mathbf{x},\mathbf{x}')=\int d\mathbf{q}d\mathbf{q}'e^{(i/\hbar)(\mathbf{p}\cdot\mathbf{q}+\mathbf{p}'\cdot\mathbf{q}')}\left\langle \mathbf{r}-\frac{\mathbf{q}}{2}|\hat{A}|\mathbf{r}'-\frac{\mathbf{q}'}{2}\right\rangle\times\left\langle \mathbf{r}+\frac{\mathbf{q}}{2}|\hat{B}|\mathbf{r}'+\frac{\mathbf{q}'}{2}\right\rangle. \tag{17}$$

Similar to the inverse relation (14), there are inverse relations for products of matrix elements. The simplest case is the inverse relation for $[AB]_d(\mathbf{x},\mathbf{x}')=A(\mathbf{x})B(\mathbf{x}')$. It is a product of two inverse formulas like Eq. (14). The inverse relations corresponding to Eq. (16) and (17) are

$$\langle \mathbf{r}_0|\hat{A}|\mathbf{r}_1\rangle\langle \mathbf{r}_2|\hat{B}|\mathbf{r}_3\rangle=\int\frac{d\mathbf{p}d\mathbf{p}'}{h^{2d}}[AB]_s(\mathbf{x},\mathbf{x}')e^{-(i/\hbar)[\mathbf{p}\cdot(\mathbf{r}_3-\mathbf{r}_0)+\mathbf{p}'\cdot(\mathbf{r}_1-\mathbf{r}_2)]} \tag{18}$$

$$=\int\frac{d\mathbf{p}d\mathbf{p}'}{h^{2d}}[AB]_c(\mathbf{x},\mathbf{x}')e^{-(i/\hbar)[\mathbf{p}\cdot(\mathbf{r}_2-\mathbf{r}_0)+\mathbf{p}'\cdot(\mathbf{r}_3-\mathbf{r}_1)]}, \tag{19}$$

where in Eq. (18) $\mathbf{x}=((\mathbf{r}_3+\mathbf{r}_0)/2,\mathbf{p})$ and $\mathbf{x}'=((\mathbf{r}_1+\mathbf{r}_2)/2,\mathbf{p}')$, while in Eq. (19) $\mathbf{x}=((\mathbf{r}_2+\mathbf{r}_0)/2,\mathbf{p})$, and $\mathbf{x}'=((\mathbf{r}_1+\mathbf{r}_3)/2,\mathbf{p}')$.

In understanding the nature of the new Wigner representations, it will be instructive to consider examples. As a first example consider the operators

$$\hat{A}=f_\sigma(\hat{\mathbf{r}}-\mathbf{r}_0)\quad\text{and}\quad\hat{B}=f_\sigma(\hat{\mathbf{r}}-\mathbf{r}_1), \tag{20}$$

where $f_\sigma(\mathbf{r})$ is a Gaussian function of width σ:

$$f_\sigma(\mathbf{r})=\frac{1}{(2\pi\sigma)^{d/2}}\exp\left\{-\frac{\mathbf{r}^2}{2\sigma}\right\}. \tag{21}$$

A straightforward calculation of the Wigner representations yields

$$[AB]_d(\mathbf{x}',\mathbf{x})=f_\sigma(\mathbf{r}-\mathbf{r}_0)f_\sigma(\mathbf{r}'-\mathbf{r}_1) \tag{22}$$

and

$$[AB]_{s,c}(\mathbf{x}',\mathbf{x}) = h^d \delta(\mathbf{r}-\mathbf{r}') f_\sigma(\mathbf{r}-\mathbf{r}_0) f_\sigma(\mathbf{r}'-\mathbf{r}_1) \times f_{\hbar^2/2\sigma}(\mathbf{p}\pm\mathbf{p}') \exp\left\{ \frac{(\mathbf{r}_1-\mathbf{r}_0)^2}{4\sigma} + \frac{i}{\hbar}(\mathbf{p}\pm\mathbf{p}') \times (\mathbf{r}_1-\mathbf{r}_0) \right\}, \quad (23)$$

where the + and − signs of $\mathbf{p}'$ correspond to $[AB]_c$ and $[AB]_s$ respectively. $[AB]_d(\mathbf{x}',\mathbf{x})$ is independent of the momenta and large when $\mathbf{r}\sim\mathbf{r}_0$ and $\mathbf{r}'\sim\mathbf{r}_1$. On the other hand, $[AB]_{s,c}(\mathbf{x}',\mathbf{x})$ are exponentially small for all values of $\mathbf{x}$ and $\mathbf{x}'$, when $|\mathbf{r}_0\text{-}\mathbf{r}_1| \gg \sigma$. If $\mathbf{r}_0=\mathbf{r}_1$ and $\sigma|\mathbf{p}|^2/\hbar^2 \gg 1$, then $[AB]_{s,c}(\mathbf{x}',\mathbf{x}) \approx h^d f_\sigma^2(\mathbf{r}-\mathbf{r}_0)\,\delta(\mathbf{r}'-\mathbf{r})\,\delta(\mathbf{p}\pm\mathbf{p}')$.

As a second example consider the case

$$\hat{A}=\hat{B}=|\phi\rangle\langle\phi|. \quad (24)$$

Here both observables are equal to the same projection operator. Assuming the wave function $\phi(\mathbf{r})$ to be real (as for the case of time reversal symmetry) one immediately sees that all types of Wigner transforms are precisely the same:

$$[AA]_{s,c}(\mathbf{x}',\mathbf{x}) = [AA]_d(\mathbf{x}',\mathbf{x}) = \rho_\phi(\mathbf{x}')\rho_\phi(\mathbf{x}), \quad (25)$$

where

$$\rho_\phi(\mathbf{x}) = \int d\mathbf{q} e^{(i/\hbar)\mathbf{p}\cdot\mathbf{q}} \left\langle \mathbf{r}-\frac{\mathbf{q}}{2}\middle|\phi\right\rangle \left\langle \phi\middle|\mathbf{r}+\frac{\mathbf{q}}{2}\right\rangle \quad (26)$$

is the Wigner function of the state $\phi(\mathbf{r})$. $\rho_\phi(\mathbf{x})$ is a real function which upon small smearing in phase space yields a positive definite function that can be interpreted a ''classical'' density distribution [29].

B. One-point functions

To begin with the calculation of correlation functions, it is instructive to consider, first, the simplest case of one-point functions:

$$C_A = \langle \mathrm{Tr}\{\hat{A}\ \mathrm{Im}\, G^-(\epsilon)\}\rangle = \int \frac{d\mathbf{x}}{h^d} A(\mathbf{x}) \langle \mathrm{Im}\, G^-(\mathbf{x})\rangle. \quad (27)$$

Here $\hat{A}$ is an observable, and $\mathrm{Im}\, G^-(\epsilon)$ is the imaginary part of the retarded Green function. The second equality in the above formula is obtained by substituting Eq. (14) into the trace, and taking into account that energy averaging acts only on the Green function. This averaging leaves only the Weyl contribution (1); therefore,

$$C_A = \pi \langle\langle A(\mathbf{x})\rangle\rangle, \quad (28)$$

where double brackets denote the microcanonical average over the energy shell $\epsilon=\mathcal{H}(\mathbf{x})$, i.e.,

$$\langle\langle A(\mathbf{x})\rangle\rangle = \int \frac{d\mathbf{x}}{h^d} A(\mathbf{x})\,\delta(\epsilon-\mathcal{H}(\mathbf{x})). \quad (29)$$

Notice that $\hat{A}$ and $\langle\langle A(\mathbf{x})\rangle\rangle$ do not have the same dimensions, they differ by dimensions of energy.

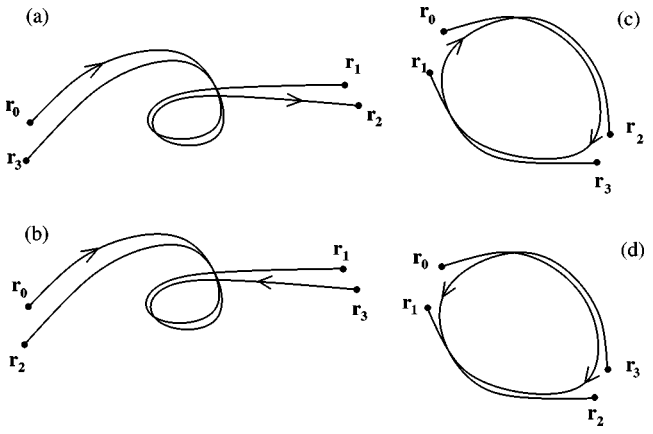

FIG. 2. The orbit configurations contributing to the average of the Green functions product $\langle G^+_{osc}(\mathbf{r}_1,\mathbf{r}_0)G^-_{osc}(\mathbf{r}_3,\mathbf{r}_2)\rangle$.

C. Two-point functions

We turn, now, to the calculation of the two-point function

$$C_{AB}(\omega) = \langle \mathrm{Tr}\{G^+(\epsilon+\hbar\omega)\hat{A}\}\mathrm{Tr}\{G^-(\epsilon)\hat{B}\}\rangle_c, \quad (30)$$

where $\langle\cdots\rangle_c$ denotes the connected part of the correlator [30]. Within the semiclassical approximation it means that only the oscillatory parts of the Green functions contribute to $C_{AB}(\omega)$. Inserting complete sets of position states one can write the correlator (30) as

$$C_{AB}(\omega) = \int d\mathbf{r}_0 d\mathbf{r}_1 d\mathbf{r}_2 d\mathbf{r}_3 A(\mathbf{r}_0,\mathbf{r}_1) B(\mathbf{r}_2,\mathbf{r}_3) \times \langle G^+_{osc}(\mathbf{r}_1,\mathbf{r}_0;\epsilon+\hbar\omega) G^-_{osc}(\mathbf{r}_3,\mathbf{r}_2;\epsilon)\rangle, \quad (31)$$

where

$$A(\mathbf{r}_0,\mathbf{r}_1) = \langle \mathbf{r}_0|\hat{A}|\mathbf{r}_1\rangle, \quad B(\mathbf{r}_2,\mathbf{r}_3) = \langle \mathbf{r}_2|\hat{B}|\mathbf{r}_3\rangle. \quad (32)$$

Next we evaluate the average of $\langle G^+_{osc}G^-_{osc}\rangle$. For this purpose notice that, to obtain a nonzero contribution, one has to pair orbits of the two Green function with similar actions. This condition imposes restrictions as for the possible configuration of the coordinates $\mathbf{r}_0,\mathbf{r}_1,\mathbf{r}_2$, and $\mathbf{r}_3$. The possibilities (in systems with time reversal symmetries) are (i) $\mathbf{r}_0 \sim \mathbf{r}_3$ and $\mathbf{r}_1\sim\mathbf{r}_2$, as illustrated in Fig. 2(a); (ii) $\mathbf{r}_0\sim\mathbf{r}_2$ and $\mathbf{r}_1\sim\mathbf{r}_3$, as shown in Fig. 2(b); and (iii) two possibilities corresponding to the cases $\mathbf{r}_0\sim\mathbf{r}_1$ and $\mathbf{r}_2\sim\mathbf{r}_3$, where the orbits are deformations of periodic orbits, as can be seen in Figs. 2(c) and 2(d). These pairing possibilities imply that the two-point function is a sum of terms

$$C_{AB}(\omega) = C^a_{AB}(\omega) + C^b_{AB}(\omega) + C^{c+d}_{AB}(\omega), \quad (33)$$

where the superscripts a, b, c, and d refer to the contributions associated with configurations of trajectories as shown in Fig. 2.

We turn to calculate the various terms of $C_{AB}(\omega)$. Consider, first, $C^a_{AB}(\omega)$ associated with the configuration of orbits shown Fig. 2(a). We start by substituting the Wigner representation (18), implied by the pairing of initial and final points, into Eq. (31). Then we change variables to

$$\mathbf{r}=(\mathbf{r}_0+\mathbf{r}_3)/2, \quad \mathbf{r}'=(\mathbf{r}_1+\mathbf{r}_2)/2,$$

$$\mathbf{q}=\mathbf{r}_3-\mathbf{r}_0, \quad \mathbf{q}'=\mathbf{r}_1-\mathbf{r}_2,$$

and perform the average over the Green functions. This average gives precisely the classical propagator $\Pi(\mathbf{x}',\mathbf{x};\omega)$ [see Eq. (5)]; therefore,

$$C^a_{AB}(\omega)=\int d\mathbf{x}d\mathbf{x}'[AB]_s(\mathbf{x},\mathbf{x}')\Pi(\mathbf{x}',\mathbf{x};\omega)$$
$$=\frac{2\pi}{\hbar}\int_0^\infty dt\, e^{i\omega t}\langle\langle[AB]_s(\mathbf{x},\mathbf{x}(t))\rangle\rangle, \qquad (34)$$

where in the second line we substitute formula (10) for $\Pi(\mathbf{x}',\mathbf{x};\omega)$, and integrate over $\mathbf{x}'$.

The calculation of the contribution, coming from orbits of the type shown in Fig. 2(b), follows along the same lines. The difference is that now we use the second Wigner representation, Eq. (19). Changing, again, variables to means and differences of the initial coordinates, and using the time reversal symmetry of the system, $G^{\pm}(\mathbf{r}_3,\mathbf{r}_2)=G^{\pm}(\mathbf{r}_2,\mathbf{r}_3)$, yields

$$C^b_{AB}(\omega)=\int d\mathbf{x}d\mathbf{x}'[AB]_c(\mathbf{x},\mathbf{x}')\Pi(\mathbf{x}',\mathbf{x};\omega)$$
$$=\frac{2\pi}{\hbar}\int_0^\infty dt\, e^{i\omega t}\langle\langle[AB]_c(\mathbf{x},\mathbf{x}(t))\rangle\rangle. \qquad (35)$$

The computation of the last two contributions, associated with the orbits of Figs. 2(c) and 2(d), requires an additional step. This step comes in order to impose the condition that the two orbits are deformations of the same periodic orbit. It is achieved by requiring that the orbit from $\mathbf{r}_0$ to $\mathbf{r}_1$ passes near $(\mathbf{r}_2+\mathbf{r}_3)/2$, and similarly the orbit from $\mathbf{r}_3$ to $\mathbf{r}_2$ passes in the vicinity of $(\mathbf{r}_0+\mathbf{r}_1)/2$. To implement this condition it will be convenient to introduce a local coordinate system $\mathbf{r}=(\tau,\mathbf{r}_\perp)$, where τ is the time along the trajectory while the coordinate $\mathbf{r}_\perp$ is perpendicular to it. Then the oscillatory part of the Green function satisfies the semiclassical product relation

$$G^{\pm}_{osc}(\mathbf{r}_1,\mathbf{r}_0;\epsilon)\simeq\hbar\int \dot{r}\, d\mathbf{r}_\perp G^{\pm}_{osc}(\mathbf{r}_1,\mathbf{r};\epsilon)G^{\pm}_{osc}(\mathbf{r},\mathbf{r}_0;\epsilon). \qquad (36)$$

This relation can be proved by calculating the integral in the stationary phase approximation; see Appendix C.

Substituting Eq. (36) in Eq. (31) and representing the matrix elements of the operators $\hat{A}$ and $\hat{B}$ in terms of their inverse Wigner transforms [Eq. (14)], we obtain

$$C^{c+d}_{AB}(\omega)=\int d\mathbf{x}d\mathbf{x}'[AB]_d(\mathbf{x},\mathbf{x}')K(\mathbf{x}',\mathbf{x}), \qquad (37)$$

where

$$K(\mathbf{x}',\mathbf{x})=\frac{\hbar^2}{h^{2d}}\int d\mathbf{q}d\mathbf{q}'d\mathbf{r}_\perp d\mathbf{r}'_\perp \dot{r}\dot{r}' e^{-(i/\hbar)(\mathbf{p}\cdot\mathbf{q}+\mathbf{p}'\cdot\mathbf{q}')}$$
$$\times\left\langle G^+_{osc}\left(\mathbf{r}+\frac{\mathbf{q}}{2},\mathbf{r}'+\mathbf{r}'_\perp;\epsilon+\hbar\omega\right)\right.$$
$$\times G^+_{osc}\left(\mathbf{r}'+\mathbf{r}'_\perp,\mathbf{r}-\frac{\mathbf{q}}{2};\epsilon+\hbar\omega\right)$$
$$\times G^-_{osc}\left(\mathbf{r}'+\frac{\mathbf{q}'}{2},\mathbf{r}+\mathbf{r}_\perp;\epsilon\right)$$
$$\left.\times G^-_{osc}\left(\mathbf{r}+\mathbf{r}_\perp,\mathbf{r}'-\frac{\mathbf{q}'}{2};\epsilon\right)\right\rangle,$$

$\mathbf{x}=(\mathbf{r},\mathbf{p})$, and $\mathbf{x}'=(\mathbf{r}',\mathbf{p}')$. In obtaining the above integral we also changed variables to

$$\mathbf{r}=(\mathbf{r}_0+\mathbf{r}_1)/2, \quad \mathbf{r}'=(\mathbf{r}_2+\mathbf{r}_3)/2,$$

$$\mathbf{q}=\mathbf{r}_1-\mathbf{r}_0, \quad \mathbf{q}'=\mathbf{r}_3-\mathbf{r}_2.$$

Now we approximate the average of the four Green functions by the diagonal approximation. Diagonal sums in this case can be formed in two ways coming from the two possibilities of pairing the retarded and advanced Green functions. These two possibilities correspond to the orbits configurations illustrated in Figs. 2(c) and 2(d). The two contributions are identical due to the time reversal symmetry of our system. As in the calculation of the classical propagator, we expand the actions to linear order around $\mathbf{r}$, $\mathbf{r}'$, and ϵ, and integrate over $\mathbf{q}$, $\mathbf{q}'$, $\mathbf{r}_\perp$, and $\mathbf{r}'_\perp$. The result is

$$K(\mathbf{x}',\mathbf{x})=8\pi^2\hbar^{2d}\dot{r}\dot{r}'\sum_{\mu\nu}|A_\mu|^2|A_\nu|^2 e^{i\omega(t_\mu+t_\nu)}$$
$$\times\delta\left(\mathbf{p}-\frac{\mathbf{p}_\mu+\mathbf{p}_\nu}{2}\right)\delta(\mathbf{p}_{\mu\perp}-\mathbf{p}_{\nu\perp})$$
$$\times\delta\left(\mathbf{p}'-\frac{\mathbf{p}'_\mu+\mathbf{p}'_\nu}{2}\right)\delta(\mathbf{p}'_{\mu\perp}-\mathbf{p}'_{\nu\perp}),$$

where t_μ and t_ν are the periods of the orbits going from $\mathbf{r}$ to $\mathbf{r}'$ and from $\mathbf{r}'$ to $\mathbf{r}$, respectively. $\mathbf{p}_\mu$ and $\mathbf{p}_\nu$ denote the momenta of the orbits at $\mathbf{r}$, and similarly $\mathbf{p}'_\mu$ and $\mathbf{p}'_\nu$ are the momenta at $\mathbf{r}'$. We denote by subscript $\perp$ the perpendicular components of momenta that are conjugate to $\mathbf{r}_\perp$. Finally, we replace the sum over orbits by an integral using the sum rule (9), and obtain

$$C^{c+d}_{AB}(\omega)=2\int\frac{dtdt'}{\hbar^2}e^{i\omega(t+t')}\langle\langle[AB]_d(\mathbf{x},\mathbf{x}')\rangle\rangle_{t,t'}. \qquad (38)$$

The average $\langle\langle\cdots\rangle\rangle_{t,t'}$ of a general function $g(\mathbf{x},\mathbf{x}')$ is defined as

$$\langle\langle g(\mathbf{x},\mathbf{x}')\rangle\rangle_{t,t'} = \int d\mathbf{x}d\mathbf{x}' g(\mathbf{x},\mathbf{x}')\,\delta(\epsilon-\mathcal{H}(\mathbf{x}))\,\delta(\epsilon - \mathcal{H}(\mathbf{x}'))\,\delta(\mathbf{x}'_{\parallel}-\mathbf{x}_{\parallel}(t))\,\delta(\mathbf{x}_{\parallel}-\mathbf{x}'_{\parallel}(t')), \tag{39}$$

where $\mathbf{x}_{\parallel}$ denote a coordinate on the energy shell $\epsilon=\mathcal{H}(\mathbf{x})$. The two δ functions in the above integral imply that the average is over periodic orbits on the energy shell with period $t+t'$. The factor of 2 in Eq. (38) is due to the time reversal symmetry.

The final result for the two-point function, $C_{AB}(\omega)$, is the sum [Eq. (33)] of Eqs. (34), (35), and (38). It expresses a quantum mechanical quantity, in terms of classical correlation functions associated with the Wigner representations of the operators $\hat{A}$ and $\hat{B}$. There are two sources of contributions to $C_{AB}(\omega)$: open trajectories, and periodic orbits. The magnitude of the corresponding terms depends on properties of the various Wigner representations $[AB]_d(\mathbf{x},\mathbf{x}')$, $[AB]_s(\mathbf{x},\mathbf{x}')$, and $[AB]_c(\mathbf{x},\mathbf{x}')$. When $A(\mathbf{x})$ and $B(\mathbf{x}')$ are very smooth functions, the main contribution comes from periodic orbits. If, on the other hand, $\hat{A}$ and $\hat{B}$ equal to the same projector, the main contribution comes from open orbits.

D. Diagrams rules for *n*-point functions in systems with time reversal symmetry

The results for the two-point function can be generalized to *n*-point functions in systems with time reversal symmetry. It is instructive to formulate this generalization in terms of a set of rules for a diagrammatic calculation. Only the connected part of the correlation functions will be considered here. It implies that the relevant part of the Green function is the oscillatory contribution (2).

We define the dimensionless propagator on the energy surface as

$$\Pi_{\epsilon}(\mathbf{x}'_{\parallel},\mathbf{x}_{\parallel};\omega) = \frac{2\pi}{\hbar}\int_0^{\infty} dt\;\; e^{i\omega t} h^d \delta(\mathbf{x}'_{\parallel}-\mathbf{x}_{\parallel}(t)), \tag{40}$$

where both $\mathbf{x}_{\parallel}$ and $\mathbf{x}'_{\parallel}$ lie on the energy shell $\epsilon=\mathcal{H}(\mathbf{x})$. In order to shorten our notations, from now on, we omit the subscript $\parallel$. The rules for calculating the average of an *n*-point functions are the following.

(i) Write the correlation function as a space integral involving the matrix elements of the operators and the Green functions.

(ii) Find all possible pairs of initial and final points connected by Green functions, and construct the orbits configurations as in Fig. 2. To each coordinate pair assign a phase space point.

(iii) Express the matrix elements of the operators as an inverse transform of the Wigner representation implied by the pairing configuration of the initial and final points. These Wigner representation are functions of the phases space points assigned in step (ii).

(iv) Phase space points connected by retarded and advanced Green functions are associated with the classical propagator (40) connecting the two points.

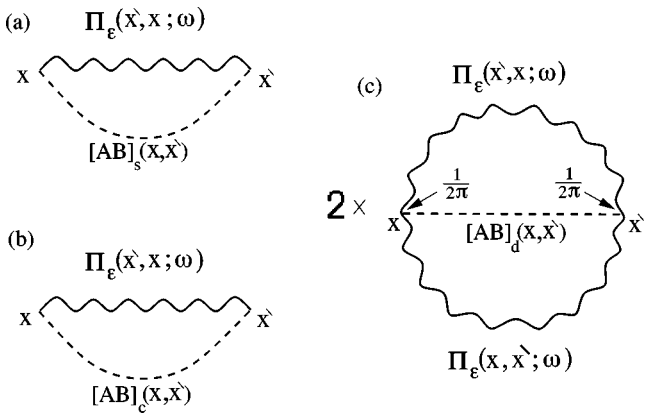

FIG. 3. The diagrams of the two-point function $C_{AB}(\omega)$. Wiggly lines represent the classical propagator on the energy shell [Eq. (40)], and the dashed line correspond to the verticies given by the appropriate Wigner representation of the observables $\hat{A}$ and $\hat{B}$.

(v) In the case where two classical propagators join at the same phase space point, then such a point is accompanied by factor of $1/2\pi$ [this factor emerges from expansions like Eq. (36)].

(vi) Integrate over all phase space coordinates with the weight $\int d\mathbf{x}\delta(\epsilon-\mathcal{H}(\mathbf{x}))(\cdots)/h^d$. This integration is the same as microcanonical averaging (29).

The diagrams of the two-point correlation function $C_{AB}(\omega)$ are shown in Fig. 3. The contributions $C^a_{AB}(\omega)$ and $C^b_{AB}(\omega)$ are represented by Figs. 3(a) and 3(b), respectively. These terms came from orbits configurations shown in Figs. 2(a) and 2(b). The two other contributions [Figs. 2(c) and 2(d)], $C^{c+d}_{AB}(\omega)$, are represented by the diagram of Fig. 3(c).

In Fig. 4 we show examples of diagrams contributing to the three-point correlation function,

$$C_{ABC}(\omega_1,\omega_2) = \langle \mathrm{Tr}\{G^+(\epsilon+\hbar\omega_1)\hat{A}\} \times \mathrm{Tr}\{G^-(\epsilon+\hbar\omega_2)\hat{B}\}\mathrm{Tr}\{G^-(\epsilon)\hat{C}\}\rangle_c . \tag{41}$$

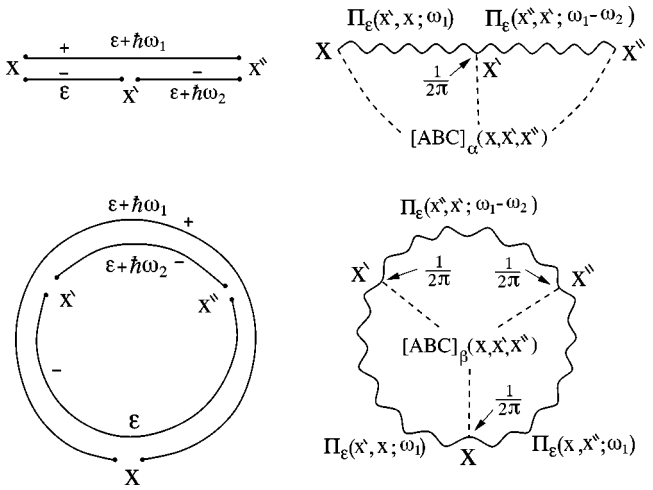

FIG. 4. Examples of diagrams contributing to the three-point function (41). The orbits configuration corresponding to a diagram is drawn on its left side. $[ABC]_{\alpha,\beta}(\mathbf{x},\mathbf{x}',\mathbf{x}'')$ denote various Wigner representations of the external product of observables, $\hat{A}\otimes\hat{B}\otimes\hat{C}$.

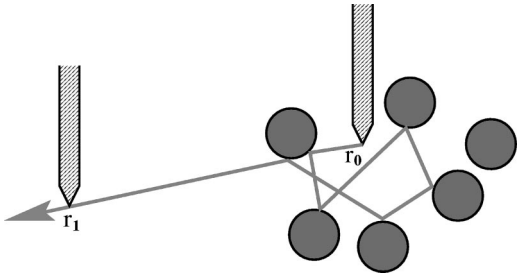

FIG. 5. An illustration of the classical N-disk scattering system. In the experimental realization of the quantum analogue of this system, using microwave cavities, a transmiter located at $\mathbf{r}_0$ excites a microwave field which is probed at $\mathbf{r}_1$.

For instance, the top diagram of this figure is equal to $\langle\langle \Pi_\epsilon(\mathbf{x}'',\mathbf{x}',\omega_1-\omega_2)\Pi_\epsilon(\mathbf{x}',\mathbf{x},\omega_1)[ABC]_\alpha(\mathbf{x},\mathbf{x}',\mathbf{x}'')\rangle\rangle/2\pi$, where the microcanonical average is with respect to all the phase space coordinates.

Finally, we remark that the procedure outlined above generates a large number of diagrams. However, knowing some general properties of the observables, such as symmetries and the smoothness of their Wigner representations, can help in reducing the number of diagrams considerably.

IV. APPLICATIONS

The purpose of this section is to present applications of the formalism developed above. In the first example we consider the N-disk scattering system [31,32]. In the second application we study the indirect photodissociation process of complex molecules [1]. Special attention will be given to understand the manifestations of the individual imprints of the systems.

A. N-disk scattering system

Consider a quantum particle moving in a two-dimensional plain, and scattered from N disks located, say, randomly near the origin; see Fig. 5. Resonances in this system can be pictured as situations where the particle is trapped for a long time in the vicinity of the disks. A natural quantity characterizing the system is the probability of finding it in a final state $|\psi_f\rangle$ when prepared in an initial state $|\psi_i\rangle$. In the experimental realization of this system [23], using microwave cavities, a transmitor prepares the particle in a localized wave packet at $\mathbf{r}_0$, and a detector collects the particle at $\mathbf{r}_1$. The signal is proportional to $|G^+(\mathbf{r}_1,\mathbf{r}_0;\epsilon)|^2$, and its simplest statistical characteristics is the correlation function:

$$K(\omega)=\frac{\langle|G^+(\mathbf{r}_1,\mathbf{r}_0;\epsilon)|^2|G^+(\mathbf{r}_1,\mathbf{r}_0;\epsilon+\hbar\omega)|^2\rangle}{\langle|G^+(\mathbf{r}_1,\mathbf{r}_0;\epsilon)|^2\rangle^2}-1. \tag{42}$$

To implement the diagrammatic approach, we start by writing $|G^+(\mathbf{r}_1,\mathbf{r}_0;\epsilon)|^2$ as a trace:

$$|G^+(\mathbf{r}_1,\mathbf{r}_0;\epsilon)|^2=\mathrm{Tr}\{G^+(\epsilon)\delta(\hat{\mathbf{r}}-\mathbf{r}_0)G^-(\epsilon)\delta(\hat{\mathbf{r}}-\mathbf{r}_1)\}. \tag{43}$$

The orbit configuration representing the above formula is shown in Fig. 6(a). Assuming the distance $|\mathbf{r}_1-\mathbf{r}_0|$ to be larger than the particle wavelength, there will be only one

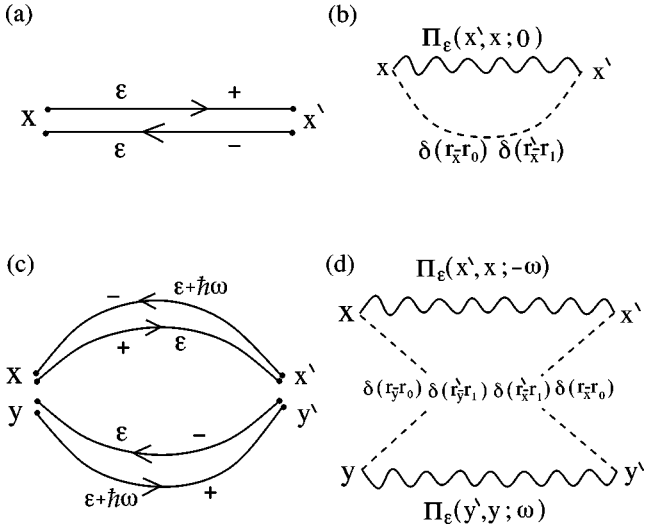

FIG. 6. The diagrams of the correlation function $K(\omega)$. (a) The orbit configuration, and (b) the corresponding diagram for $\langle|G^+(\mathbf{r}_1,\mathbf{r}_0;\epsilon)|^2\rangle$. (c) The orbit configuration, and (d) the diagram for the connected part of $\langle|G^+(\mathbf{r}_1,\mathbf{r}_0;\epsilon)|^2|G^+(\mathbf{r}_1,\mathbf{r}_0;\epsilon+\hbar\omega)|^2\rangle$.

contribution associated with the oscillatory parts of the Green functions. The diagram representing this contribution is shown in Fig. 6(b). A straightforward calculation of this diagram yields

$$\langle|G^+(\mathbf{r}_1,\mathbf{r}_0;\epsilon)|^2\rangle=\int_0^\infty dt\, f(\mathbf{r}_1,\mathbf{r}_0;t), \tag{44}$$

where

$$f(\mathbf{r}_1,\mathbf{r}_0;t)=\int\frac{d\mathbf{p}_0}{h^{d-1}\hbar^2}\delta(\epsilon-\mathcal{H}(\mathbf{x}_0))\delta(\mathbf{r}_1-\mathbf{r}(\mathbf{x}_0,t)) \tag{45}$$

is proportional to the classical probability of finding particle at $\mathbf{r}_1$, starting from $\mathbf{r}_0$ in all possible directions, and evolving according to the classical equations of motion. Here $\mathbf{r}(\mathbf{x}_0,t)$ denotes the trajectory of the particle, as function of time t, starting from the initial phase space point $\mathbf{x}_0=(\mathbf{r}_0,\mathbf{p}_0)$.

The correlator $K(\omega)$ is proportional to the diagram shown in Fig. 6(d), where again we assume the distance between $\mathbf{r}_1$ and $\mathbf{r}_0$ to be much longer than the particle wavelength. A straightforward calculation of this diagram leads to

$$K(\omega)=\left|\frac{F(\mathbf{r}_1,\mathbf{r}_0;\omega)}{F(\mathbf{r}_1,\mathbf{r}_0;0)}\right|^2, \tag{46}$$

where

$$F(\mathbf{r}_1,\mathbf{r}_0;\omega)=\int_0^\infty dt\;\; e^{i\omega t}f(\mathbf{r}_1,\mathbf{r}_0;t) \tag{47}$$

is the Fourier transform of $f(\mathbf{r}_1,\mathbf{r}_0;t)$ for time $t>0$.

In understanding the typical behavior of $K(\omega)$, it is necessary to characterize the function $f(\mathbf{r}_1,\mathbf{r}_0;t)$. The spectral decomposition of the classical propagator [Eq. (12)] implies that [33]

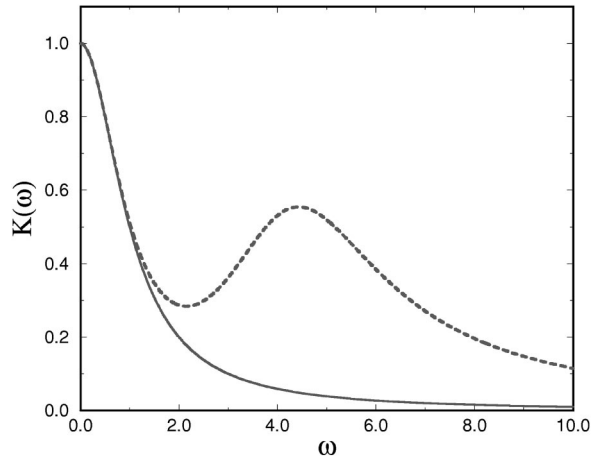

FIG. 7. The correlation function $K(\omega)$. The solid line correspond to the universal limit where $b_\alpha=0$ for all $\alpha>0$. The dotted line includes nonuniversal imprints of the system, with $b_1=1.5$, $\gamma_1'=2$, and $\gamma_1''=4$.

$$f(\mathbf{r}_1,\mathbf{r}_0;t)=\sum_\alpha b_\alpha e^{-\gamma_\alpha t}, \tag{48}$$

where γ_α are the Ruelle resonances of the system, and b_α are coefficients associated with the eigenfunctions of the classical propagator, $\chi_\alpha^l(\mathbf{x})$ and $\chi_\alpha^r(\mathbf{x})$, as well as the precise positions of the transmitor and the detector. The first eigenvalue γ_0 is the escape rate of the system. This eigenvalue dominates the behavior of the system at long times, i.e. small ω. Taking only its contribution, the correlation function reduces to a Lorentzian, $K(\omega)\approx\gamma_0^2/(\gamma_0^2+\omega^2)$. This result has been known long ago in nuclear physics [2]. It was reproduced in the context of chaotic scattering [34–36], and also measured experimentally in a microwave cavities [37].

We turn to a consideration of the nonuniversal imprints of the system on $K(\omega)$. For this purpose we shall take into account contributions of higher Ruelle resonances in Eq. (48). It will be convenient to rescale all frequencies with γ_0, and set $b_0=1$ (without loss of generality). Then, adding the next term of eq. (48), $F(\omega)$ takes the form

$$F(\omega)\simeq\frac{1}{1+i\omega}+\sum_{\pm}\frac{b_1}{\gamma_1'+i(\omega\pm\gamma_1'')}, \tag{49}$$

where γ_1' and γ_1'' denote the real and the imaginary parts of γ_1, respectively, and we assume b_1 to be real. In Fig. 7 we plot the correlation function $K(\omega)$ calculated from Eq. (46) using Eq. (49). The solid line is the Lorentzian obtained when $b_\alpha=0$ for $\alpha>0$. The dashed line is a representative example of the nonuniversal behavior of the system (with $b_1=1.5$, $\gamma_1'=2$, $\gamma_1''=4$, and $b_\alpha=0$ for $\alpha>1$).

A behavior very similar to that shown in Fig. 7 was recently observed in a microwave experiment on the four-disk system [23]. Our results explain the additional peak in the measured correlation function, $K(\omega)$, as an imprint of the complex Ruelle resonances of the system [38].

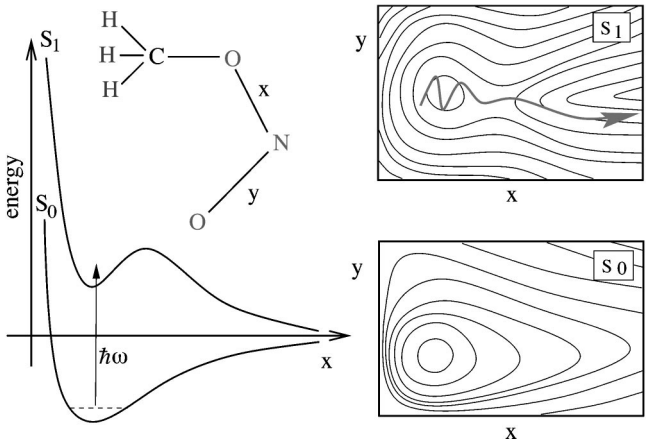

FIG. 8. An illustration for the electronic energy surfaces of methyl nitrite, CH_3ONO, as an example for a complex molecule which undergoes an indirect photodissociation process. S_0 and S_1 are contour plots of the electronic surface potential associated with the ground and the excited electronic states. They are plotted as functions of the distances between the nitrogen and the oxygen atoms, keeping all other degrees of freedom fixed at their equilibrium values. The irregular shape of S_1 leads to chaotic dynamics of the excited molecule.

B. Statistics of photodissociation spectra

As a second application of the semiclassical diagrammatic approach, we study the statistics of photodissociation spectra of complex molecules, such as the radicals HO_2 and NO_2. Disintegration of such molecules is a two-step process. In the first step, a photon excites the molecule to an energy above the dissociation threshold. Then fragmentation proceeds by redistribution of energy in the vibrational degrees of freedom, or tunneling from binding to unbinding energy surfaces of the adiabatic electronic potential [1]. A barrier, which separates quasistable states from continuum modes, hinders the immediate dissociation of the excited molecule. The large number of degrees of freedom and the complexity of the system imply that, on these long lived resonances, the dynamics of the system is chaotic. An illustration of such a system is depicted in Fig. 8.

Consider a molecule, in the ground state $|g\rangle$, excited by a light pulse to an energy above the dissociation threshold, and let $\hat{\mathcal{H}}$ denote the Hamiltonian of the system on the excited electronic surface (S_1 in the illustration of Fig. 8). It will be assumed that $\hat{\mathcal{H}}$ represents an open system with several open channels. The photodissociation cross section of the molecule, in the dipole approximation, is given by

$$\sigma(\epsilon)=\eta\,\mathrm{Im\,Tr}\{\hat{A}G^-(\epsilon)\}, \tag{50}$$

where $G^-(\epsilon)$ is the retarded Green function of the molecule, and $\hat{A}$ is a projection operator given by

$$\hat{A}=|\phi\rangle\langle\phi| \quad \text{where } |\phi\rangle=\mathcal{D}|g\rangle. \tag{51}$$

Here $\mathcal{D}=\mathbf{d}\cdot\hat{\mathbf{e}}$ is the projection of the electronic dipole moment operator of the molecule $\mathbf{d}$, on the polarization $\hat{\mathbf{e}}$, of the absorbed light, and $\eta=\epsilon/c\hbar\varepsilon_0$, c being the speed of light,

and ε_0 the electric permitivity. The energy ϵ is measured from the ground state of the molecule.

A natural statistical characteristic of the photodissociation process is the dimensionless two-point correlation function:

$$Z(\omega)=\frac{\langle\sigma(\epsilon)\sigma(\epsilon+\hbar\omega)\rangle_c}{\langle\sigma(\epsilon)\rangle^2}. \tag{52}$$

It will be assumed that the excitation energy, ϵ, is sufficiently high such that the mean spacing between the vibrational modes of the molecule is smaller than the energy broadening due to the finite lifetime of the system in the excited states. This is the regime of overlapping resonances.

From Eqs. (50), (27), and (30) it follows that the correlation function (52) is equal to

$$Z(\omega)=\frac{1}{2}\mathrm{Re}\frac{C_{AA}(\omega)}{C_A^2}, \tag{53}$$

where $\hat{A}$ is the projection operator [Eq. (51)], while C_A and $C_{AA}(\omega)$ are the corresponding one- and two-point functions. The special feature of the operator $\hat{A}\otimes\hat{A}$ is that all its Wigner representations are identical; see Eq. (25). This implies that Eq. (53) has the form

$$Z(\omega)\simeq Z_1(\omega)+Z_2(\omega), \tag{54}$$

where $Z_1(\omega)$ is the contribution of open orbits [Figs. 2(a) and 2(b)],

$$Z_1(\omega)=\frac{2}{\pi\hbar}\mathrm{Re}\int_0^\infty dt\, e^{i\omega t}\ \frac{\langle\langle\rho_\phi(\mathbf{x}(t))\rho_\phi(\mathbf{x})\rangle\rangle}{\langle\langle\rho_\phi(\mathbf{x})\rangle\rangle^2}, \tag{55}$$

while $Z_2(\omega)$ is the contribution of periodic orbits [Figs. 2(c) and 2(d)]:

$$Z_2(\omega)=\frac{1}{\pi^2\hbar^2}\mathrm{Re}\int_0^\infty dtdt'\, e^{i\omega(t+t')}\frac{\langle\langle\rho_\phi(\mathbf{x})\rho_\phi(\mathbf{x}')\rangle\rangle_{t,t'}}{\langle\langle\rho_\phi(\mathbf{x})\rangle\rangle^2}. \tag{56}$$

$\rho_\phi(\mathbf{x})$ in the above formulas is the Wigner function of the initial state $\mathcal{D}|g\rangle$.

Consider the limit of small ω. This limit reflects the long time behavior of the correlation functions $\langle\langle\rho_\phi(\mathbf{x}(t))\rho_\phi(\mathbf{x})\rangle\rangle$ and $\langle\langle\rho_\phi(\mathbf{x})\rho_\phi(\mathbf{x}')\rangle\rangle_{t,t'}$. The leading contribution, in this case, comes from the smallest eigenvalue in the spectral decomposition (12), i.e. γ_0. Taking into account only this eigenvalue, we obtain

$$\langle\langle\rho_\phi(\mathbf{x}(t))\rho_\phi(\mathbf{x})\rangle\rangle\simeq ae^{-\gamma_0 t},$$

$$\langle\langle\rho_\phi(\mathbf{x})\rho_\phi(\mathbf{x}')\rangle\rangle_{t,t'}\simeq be^{-\gamma_0(t+t')},$$

where

$$a=h^d\langle\langle\rho_\phi(\mathbf{x})\chi_0^l(\mathbf{x})\rangle\rangle\langle\langle\rho_\phi(\mathbf{x})\chi_0^r(\mathbf{x})\rangle\rangle, \tag{57}$$

$$b=h^{2d}\langle\langle\rho_\phi(\mathbf{x})\chi_0^l(\mathbf{x})\chi_0^r(\mathbf{x})\rangle\rangle^2. \tag{58}$$

The ratio $b/a=\Delta$ has an energy dimension. In the semiclassical limit $\hbar\to 0$, it approaches zero as $\hbar^d$; thus it corresponds to the mean spacing between resonances. Substituting the above approximations of the classical correlation functions into Eqs. (55) and (56), and rescaling the energies as $\hbar\omega=\Omega\Delta$ and $\hbar\gamma_0=\Gamma\Delta$, one obtains

$$Z(\Omega)\approx Z^{(0)}(\Omega)=\frac{2\xi}{\pi}\left(\frac{\Gamma}{\Gamma^2+\Omega^2}+\frac{1}{2\pi}\frac{\Gamma^2-\Omega^2}{(\Gamma^2+\Omega^2)^2}\right), \tag{59}$$

where $\xi=(a/\langle\langle\rho_\phi\rangle\rangle)^2/b$ is a dimensionless constant of order unity. The first term in the brackets comes from $Z_1(\omega)$, i.e., from open trajectories of the type shown in Figs. 2(a) and 2(b). This term constitutes the leading contribution to $Z(\omega)$ when $\Gamma>1$. In the limit $\Gamma\ll 1$, the second term in the brackets becomes dominant. This term, associated with $Z_2(\omega)$, comes from the periodic orbits of the system. Notice, however, that the regime $\Gamma\ll 1$, corresponding to less than one open channel, is beyond our semiclassical approximation.

Equation (59) represents the universal limit of the correlator $Z(\Omega)$. It was first derived by Fyodorov and Alhassid [21] using the nonlinear σ model [39]. Our derivation confirms their conjecture that, in the limit of overlapping resonances ($\Gamma>1$), $Z(\omega)$ can be derived by semiclassical methods. An alternative derivation of Eq. (59), using random matrix theory, is presented in Appendix D.

The range of validity of formulas (54)–(56) goes far beyond the universal regime. They also account for system specific contributions which contain valuable information about the nature of the system. These individual imprints come from the higher eigenvalues and eigenvectors of the classical propagator [Eq. (12)].

For example, the leading nonuniversal contribution coming from $Z_1(\omega)$ is given by

$$Z_1^{(1)}(\Omega)\simeq\frac{2\xi a_1}{\pi}\sum_{\pm}\frac{\Gamma_1}{\Gamma_1^2+(\Omega\pm\Omega_1)^2}.$$

Here $\Gamma_1=\hbar\gamma_1'/\Delta$ and $\Omega_1=\hbar\gamma_1''/\Delta$, where γ_1' and γ_1'' are the real and imaginary parts of the second Ruelle resonance. The constant a_1 comes from an integral similar to Eq. (57) but with the eigenfunctions $\chi_1^{l,r}(\mathbf{x})$.

Similarly, the leading nonuniversal contribution of $Z_2(\Omega)$ is

$$Z_2^{(1)}(\Omega)\simeq\frac{2\xi b_{01}}{\pi^2}\sum_{\pm}\frac{\Gamma\Gamma_1-\Omega(\Omega\pm\Omega_1)}{(\Gamma^2+\Omega^2)(\Gamma_1^2+(\Omega\pm\Omega_1)^2)},$$

where b_{01} is a constant depending on $\rho_\phi(\mathbf{x})$ and the eigenfunctions $\chi_0^{l,r}(\mathbf{x})$ and $\chi_1^{l,r}(\mathbf{x})$.

The two-point function $Z(\Omega)$, in the approximation

$$Z(\Omega)\simeq Z^{(0)}(\Omega)+Z_1^{(1)}(\Omega)+Z_2^{(1)}(\Omega), \tag{60}$$

is plotted in Fig. 9. The solid line represents the universal form $Z^{(0)}(\Omega)$ given by Eq. (59). The dotted line shows the typical behavior of systems where decay of correlations is of diffusive nature. It appears when the subleading Ruelle resonances are purely real ($\Omega_1=0$). In this case the deviation from $Z^{(0)}(\Omega)$ appears mainly as an increase of correlations near $\Omega=0$. The dashed line corresponds to the case of a

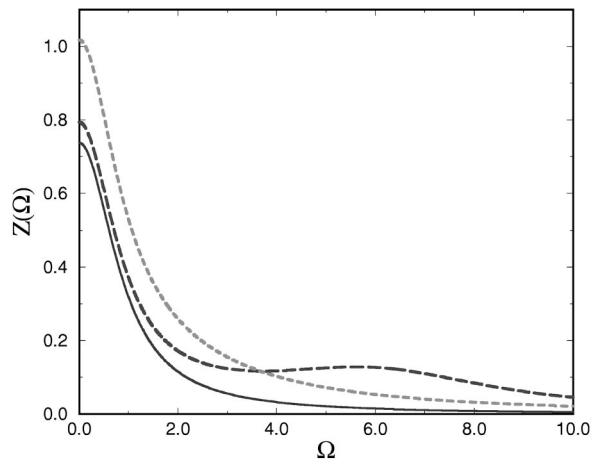

FIG. 9. The two-point function $Z(\Omega)$ of the photodissociation cross section for systems with time reversal symmetry. The solid line is the universal result [Eq. (59)] for the case $\xi=\Gamma=1$. The dashed and dotted lines show the two-point function which includes system specific contributions in the approximation of Eq. (60). In both cases $\Gamma=1$, $\Gamma_1=3$, and $a_1=b_{01}=1$, but the dashed line corresponds to $\Omega_1=6$, and the dotted line to $\Omega_1=0$.

complex Ruelle resonance ($\Omega_1\neq 0$). It characterizes the behavior of ballistic systems. Here the nonuniversal contribution is located in the tail of $Z(\Omega)$, near $\Omega=\Omega_1$, where the universal term (59) is already negligible. These plots demonstrate the significance of the individual imprints of the system on $Z(\Omega)$.

V. SUMMARY

The main result of this paper is the construction of a diagrammatic approach for calculating the *n*-point functions of open chaotic systems with time reversal symmetry. In essence, this approach is simply an economic way for evaluating the ''diagonal approximation'' for the *n*-point functions. The result is expressed in terms of classical correlation functions associated with the observables. These correlation functions reflect properties of the Perron-Frobenius spectral decomposition of the system, i.e., features of the irreversible dynamics of probability densities on the energy shell. An important ingredient of this formalism is the generalization of Wigner transforms for external products of operators.

The strength of this formalism is in its capability of treating particular systems rather than an ensemble of them. Nevertheless, in the appropriate limit, our results reduce to those of random matrix theory. This was demonstrated by considering two examples: the *N*-disk scattering system, and the process of indirect photodissociation in complex molecules. The weakness of this diagrammatic approach is the lack of a clear systematic procedure for calculating quantum corrections such as weak localization correction. This limits our treatment to systems with an escape rate sufficiently large so that the system disintegrate before weak localization effects set in.

The focus of this paper was on systems with time reversal symmetry, and no other discrete symmetries. Within the universal limit, a generalization of our results to a system without time reversal symmetry is straightforward. However, when considering nonuniversal manifestations, the situation is more complicated. The reason for this is that, usually in ballistic systems, there is no separation between the time scales on which nonuniversal features appear, and that where time reversal symmetry is broken. Further development of this diagrammatic approach should include a prescription for calculating weak localization corrections, generalization to systems without time reversal symmetry, and generalization to systems with other discrete symmetries, such as reflection or inversion.

ACKNOWLEDGMENTS

This work was initiated during the workshop on *Dynamics of Complex Systems* which took place at the Max Plank Institute in Dresden, 1999. I thank the organizers and the institute for their generous hospitality.

APPENDIX A: LOCAL TERM $\Pi_{loc}(\mathbf{x}',\mathbf{x};\omega)$.

In this appendix we calculate the Weyl contribution to the classical propagator, $\Pi(\mathbf{x}',\mathbf{x};\omega)$. Substituting Eq. (1) in Eq. (5), and integrating over $\mathbf{q}$ and $\mathbf{q}'$, we obtain

$$\Pi_{loc}(\mathbf{x}',\mathbf{x};\omega)=\int \frac{d\mathbf{p}_0 d\mathbf{p}_1}{h^{2d}}\,\delta\!\left(\mathbf{p}-\frac{\mathbf{p}_0+\mathbf{p}_1}{2}\right)\delta(\mathbf{p}-\mathbf{p}') \times\frac{e^{(i/\hbar)(\mathbf{p}_0-\mathbf{p}_1)\cdot(\mathbf{r}'-\mathbf{r})}}{[\epsilon+\hbar\omega+i0-\mathcal{H}(\mathbf{x}_0)][\epsilon-i0-\mathcal{H}(\mathbf{x}_1)]},$$

where $\mathbf{x}_0=((\mathbf{r}+\mathbf{r}')/2,\mathbf{p}_0)$, and $\mathbf{x}_1=((\mathbf{r}+\mathbf{r}')/2,\mathbf{p}_1)$. Next we change variables to $\mathbf{k}'=(\mathbf{p}_0+\mathbf{p}_1)/2$ and $\mathbf{k}=\mathbf{p}_0-\mathbf{p}_1$, and integrate over $\mathbf{k}'$. The above integral then reduces to

$$\int \frac{d\mathbf{k}}{h^{2d}}\,\frac{\delta(\mathbf{p}-\mathbf{p}')e^{(i/\hbar)\mathbf{k}\cdot(\mathbf{r}'-\mathbf{r})}}{[\epsilon+\hbar\omega+i0-\mathcal{H}(\mathbf{x}^+)][\epsilon-i0-\mathcal{H}(\mathbf{x}^-)]},$$

where $\mathbf{x}^{\pm}=((\mathbf{r}+\mathbf{r}')/2,\mathbf{p}\pm\mathbf{k}/2)$. In the semiclassical limit, $\hbar\to 0$, the integral over $\mathbf{k}$ yields a δ function; thus

$$\Pi_{loc}(\mathbf{x}',\mathbf{x};\omega)\simeq\frac{\delta(\mathbf{x}'-\mathbf{x})/h^d}{(\epsilon+\hbar\omega+i0-\mathcal{H}(\mathbf{x}))(\epsilon-i0-\mathcal{H}(\mathbf{x}))}. \tag{A1}$$

To extract the leading order semiclassical approximation of this expression, we manipulate the denominator as

$$\begin{aligned}\mathcal{D}&=\frac{1}{\hbar\omega+i0}\left[\frac{1}{\epsilon-i0-\mathcal{H}(\mathbf{x})}-\frac{1}{\epsilon+\hbar\omega+i0-\mathcal{H}(\mathbf{x})}\right]\\&\simeq\frac{1}{\hbar\omega+i0}\left[\frac{1}{\epsilon-i0-\mathcal{H}(\mathbf{x})}-\frac{1}{\epsilon+i0-\mathcal{H}(\mathbf{x})}\right]\\&=\frac{1}{\hbar\omega+i0}\,2\pi i\,\delta(\epsilon-\mathcal{H}(\mathbf{x})).\end{aligned}$$

Substituting these results in Eq. (A1), we obtain Eq. (6).

APPENDIX B: THE CLASSICAL SUM RULE (9)

In this appendix we derive the sum rule (9). The derivation will be performed by calculating the right hand side (rhs) of the equation and showing it equals to the left hand

side. It is convenient to introduce a local coordinate system with time coordinate, τ, along the trajectory, and $\mathbf{r}_\perp$ perpendicular to the trajectory. The corresponding conjugate momenta are the Hamiltonian function H, and $\mathbf{p}_\perp$. In these coordinates the rhs of formula (9) takes the form

$$[\text{rhs of Eq. (9)}]=\int_0^\infty dt \int \frac{dH dH'}{\dot{r}\dot{r}'} d\mathbf{p}_\perp d\mathbf{p}'_\perp g(\mathbf{x},\mathbf{x}',t) \times \delta(\epsilon-H')\,\delta(H-H'_t)\,\delta(\tau-\tau'_t) \times \delta(\mathbf{r}_\perp-\mathbf{r}'_{\perp t})\,\delta(\mathbf{p}_\perp-\mathbf{p}'_{\perp t}).$$

where $\dot{r}'$ and $\dot{r}$ are the absolute values of the velocity at the initial and final points, respectively, while the subscript t denotes the value of the corresponding coordinate after time t. Thus, in particular, $\mathbf{r}'_{\perp t}$ and $\mathbf{p}'_{\perp t}$ are functions of the initial phase space point $\mathbf{x}'=(\mathbf{r}',\mathbf{p}')$ and the time t. Since energy is conserved, one has $H'_t=H'$. The factor $1/\dot{r}\dot{r}'$ in the above integral comes from the Jacobian of the transformation of variables. An integration over H, H', and $\mathbf{p}_\perp$ gives

$$[\text{rhs of Eq. (9)}]=\int_0^\infty dt \int \frac{d\mathbf{p}'_\perp}{\dot{r}\dot{r}'}\,\delta(\tau-\tau'_t)\,\delta(\mathbf{r}_\perp-\mathbf{r}'_{\perp t}) \times g(\mathbf{x},\mathbf{x}',t)|_{H=H'=\epsilon,\ \mathbf{p}_\perp=\mathbf{p}'_{\perp t}}.$$

Since the initial and final points of the particle as well as its energy are fixed, there is only a discrete set of trajectories which contribute to the above integral. These are the trajectories for which $\mathbf{p}'_\perp$ takes a value such that $\mathbf{r}_\perp=\mathbf{r}'_{\perp t}$. We denote these trajectories by a subscript μ. Thus $\mathbf{p}'_{\perp\mu}$ and $\mathbf{p}_{\perp\mu}$ are the initial and final momenta of the μth trajectory, and t_μ is the corresponding period. Then

$$[\text{rhs of Eq. (9)}]=\sum_\mu \int_0^\infty dt\ \delta(t-t_\mu)\int_{\Gamma_\mu}\frac{d\mathbf{p}'_\perp}{\dot{r}\dot{r}'} \times \delta(\mathbf{r}_\perp-\mathbf{r}'_{\perp t})\,g(\mathbf{x}_\mu,\mathbf{x}'_\mu,t),$$

where Γ_μ is an infinitesimal region surrounding $\mathbf{p}'_{\perp\mu}$ in the momentum space, $\mathbf{x}_\mu=(\mathbf{r},\mathbf{p}_\mu)$, and $\mathbf{x}'_\mu=(\mathbf{r}',\mathbf{p}'_\mu)$. The integral is straightforward, and the result is

$$[\text{rhs of Eq. (9)}]=\sum_\mu\ g(\mathbf{x}_\mu,\mathbf{x}'_\mu,t_\mu)\left[\frac{1}{\dot{r}\dot{r}'}\,\mathrm{Det}^{-1}\left(\frac{\partial\mathbf{r}_\perp}{\partial\mathbf{p}'_\perp}\right)\right]_\mu,$$

where all quantities in the square brackets are calculated for the μth orbit.

To see that this result is equal to the left hand side of Eq. (9), we notice that the expression in the square brackets is related to the amplitude A_μ of the semiclassical Green function [Eq. (2)] according to [25]

$$|A_\mu|^2=\frac{1}{h^{d-1}\hbar^2}\left[\frac{1}{\dot{r}\dot{r}'}\,\mathrm{Det}^{-1}\left(\frac{\partial\mathbf{r}_\perp}{\partial\mathbf{p}'_\perp}\right)\right]_\mu. \tag{B1}$$

Combining the last two equations yields the sum rule (9).

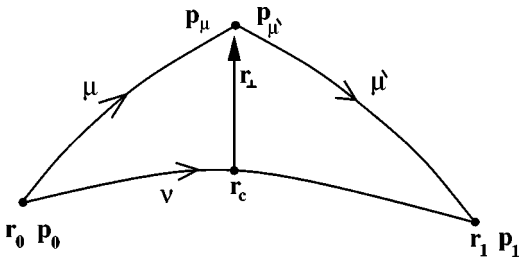

FIG. 10. Classical paths joining $\mathbf{r}_0$ $\mathbf{r}_1$ and $\mathbf{r}_c+\mathbf{r}_\perp$.

APPENDIX C: PRODUCT FORMULA EQ. (36)

In this appendix we prove the semiclassical formula (36) relating a Green function to the product of two Green functions. We consider the case of G^+_{osc}. The generalization for G^-_{osc} is straightforward. We start by evaluating the integral on the right hand side of Eq. (36) using stationary phase approximation. Substituting Eq. (2) into Eq. (36) yields

$$[\text{rhs of Eq. (36)}] =\hbar\sum_{\mu,\mu'}\int d\mathbf{r}_\perp\,\dot{r}A_\mu A_{\mu'}e^{(i/\hbar)[S_\mu(\mathbf{r}_1,\mathbf{r};\epsilon)+S_{\mu'}(\mathbf{r},\mathbf{r}_0;\epsilon)]}, \tag{C1}$$

where μ denotes the orbits from $\mathbf{r}_0$ to $\mathbf{r}$, while μ' the orbits from $\mathbf{r}$ to $\mathbf{r}_1$. The amplitudes A_μ and $A_{\mu'}$ satisfy relation (B1). The stationary phase condition of the above integral is

$$\frac{\partial}{\partial\mathbf{r}_\perp}[S_{\mu'}(\mathbf{r}_1,\mathbf{r};\epsilon)+S_\mu(\mathbf{r},\mathbf{r}_0;\epsilon)]=0.$$

With the classical relations $\partial S_\mu(\mathbf{r},\mathbf{r}_0;\epsilon)/\partial\mathbf{r}=\mathbf{p}_\mu$ and $S'_\mu(\mathbf{r}_1,\mathbf{r};\epsilon)/\partial\mathbf{r}=-\mathbf{p}'_\mu$, this implies that the momenta of the μth and μ'th trajectories at $\mathbf{r}$ are equal, $\mathbf{p}_\mu=\mathbf{p}_{\mu'}$. Thus $\mathbf{r}$ lies on a classical trajectory which goes from $\mathbf{r}_0$ to $\mathbf{r}_1$. We denote this trajectory by ν; see Fig. 10. Notice that the stationary phase condition applies only for the perpendicular components of the momenta. However, since the energy is fixed and equal for both trajectories, the longitudinal components of the momenta of both trajectories have to be equal as well.

Denoting by $\mathbf{r}_c$ a stationary value of $\mathbf{r}$, we see that the stationary phase is the action of the ν-th orbit from $\mathbf{r}_0$ to $\mathbf{r}_1$:

$$S_{\mu'}(\mathbf{r}_1,\mathbf{r}_c;\epsilon)+S_\mu(\mathbf{r}_c,\mathbf{r}_0;\epsilon)=S_\nu(\mathbf{r}_1,\mathbf{r}_0;\epsilon).$$

Thus integral (C1) takes the form

$$[\text{rhs of Eq. (36)}]=\sum_\nu\ I_\nu e^{(i/\hbar)S_\nu(\mathbf{r}_1,\mathbf{r}_0;\epsilon)},$$

where the pre-exponent factor I_ν is given by

$$I_\nu=\hbar\dot{r}A_\mu A_{\mu'}h^{(d-1)/2}\left(\mathrm{Det}\left(\frac{\partial\mathbf{p}_{\perp\mu}-\mathbf{p}_{\perp\mu'}}{\partial\mathbf{r}_\perp}\right)\right)^{-1/2}. \tag{C2}$$

This was calculated by expanding the sum of actions, $S_{\mu'}(\mathbf{r}_1,\mathbf{r};\epsilon)+S_\mu(\mathbf{r},\mathbf{r}_0;\epsilon)$ to second order in $\mathbf{r}_\perp$ around $\mathbf{r}_c$, and calculating the resulting Gaussian integral (C1).

To see the equivalence between this result and the left hand side of Eq. (36), it remains to show that $I_\nu = A_\nu$, where A_ν is the amplitude corresponding to the νth orbit from $\mathbf{r}_0$ to $\mathbf{r}_1$. It is sufficient to analyze the magnitudes of I_ν and A_ν, since the Maslov phases are additive. Substituting Eq. (B1), for A_μ and $A_{\mu'}$, in Eq. (C2) we obtain

$$I_\nu = \frac{1}{\sqrt{h^{d-1}h^2\dot{r}_0\dot{r}_1}} \left\{ \frac{\mathrm{Det}\left(\frac{\partial \mathbf{p}_{\perp\mu'}}{\partial \mathbf{r}_{\perp 1}}\right)\mathrm{Det}\left(\frac{\partial \mathbf{p}_{\perp 0}}{\partial \mathbf{r}_\perp}\right)}{\mathrm{Det}\left(\frac{\partial(\mathbf{p}_{\perp\mu}-\mathbf{p}_{\perp\mu'})}{\partial \mathbf{r}_\perp}\right)} \right\}^{1/2}.$$

Thus $I_\nu = A_\nu$ if the term in the curly brackets is equal to $\mathrm{Det}(\partial \mathbf{p}_{\perp 1}/\partial \mathbf{r}_{\perp 0})$. Following Berry and Mount [24], we first write this term as a determinant of the product of the three matrices:

$$\{\} = \mathrm{Det}\left[\left(\frac{\partial \mathbf{p}_{\perp\mu}-\mathbf{p}_{\perp\mu'}}{\partial \mathbf{r}_\perp}\right)^{-1} \times \frac{\partial \mathbf{p}_{\perp\mu'}}{\partial \mathbf{r}_{\perp 1}} \times \frac{\partial \mathbf{p}_{\perp 0}}{\partial \mathbf{r}_\perp}\right]. \quad \text{(C3)}$$

Now we use the stationary phase condition $\mathbf{p}_{\perp\mu}-\mathbf{p}_{\perp\mu'}=0$, which applies at $\mathbf{r}=\mathbf{r}_c$, and differentiate it with respect to $\mathbf{r}_{\perp 1}$, keeping $\mathbf{r}_{\perp 0}$ fixed. Then

$$\frac{\partial \mathbf{p}_{\perp\mu'}}{\partial \mathbf{r}_{\perp 1}} = \frac{\partial(\mathbf{p}_{\perp\mu}-\mathbf{p}_{\perp\mu'})}{\partial \mathbf{r}_\perp} \times \frac{\partial \mathbf{r}_\perp}{\partial \mathbf{r}_{\perp 1}}.$$

Substituting this result into Eq. (C3) and using the chain rule of derivatives, we obtain $\{\} = \mathrm{Det}(\partial \mathbf{p}_{\perp 0}/\partial \mathbf{r}_{\perp 1})$ which proves Eq. (36).

APPENDIX D: AN ALTERNATIVE DERIVATION OF EQ. (59)

In this appendix we derive formula (59) using random matrix theory [20] (RMT). Our starting point is the Hamiltonian of the form $\mathcal{H}_0 + i\gamma/2$, where $\mathcal{H}_0$ is an $N\times N$ random matrix of the Gaussian orthegonal (GOE) ensemble, and γ is a constant which equals to the typical width of the resonances. With these definitions, $\sigma(\epsilon) = \langle \phi | \delta_{\gamma/2}(\epsilon - \mathcal{H}_0) | \phi \rangle$, where

$$\delta_\gamma(x) = \frac{1}{\pi}\frac{\gamma}{\gamma^2 + x^2}, \quad \text{(D1)}$$

and $|\phi\rangle = \mathcal{D}|g\rangle$ [see Eq. (51)]. Denoting by $\varphi_\alpha(j)$ the jth component of the eigenfunction number α of $\mathcal{H}_0$, we have

$$\sigma(\epsilon) = \eta \sum_\alpha \sum_{jk} \delta_{\gamma/2}(\epsilon - \epsilon_\alpha)\varphi_\alpha(j)\varphi_\alpha(k)\phi(j)\phi(k). \quad \text{(D2)}$$

To perform the ensemble averaging we use the property of RMT that eigenenergies ϵ_α and the wave functions $\varphi_\alpha(j)$ are statistically independent. Thus

$$\langle \sigma(\epsilon) \rangle = \frac{\eta}{N\Delta} \sum_{jk} \phi(j)\phi(k)\delta_{jk},$$

where $1/\Delta = \langle \Sigma_\alpha \delta_{\gamma/2}(\epsilon - \epsilon_\alpha) \rangle$ is the average density of states, and $\langle \varphi_\alpha(j)\varphi_\alpha(k) \rangle = \delta_{jk}/N$. Working in units where $\eta \langle \phi | \phi \rangle = N$, we obtain $\langle \sigma \rangle = 1/\Delta$.

Consider now the connected part of the correlation function $\langle \sigma(\epsilon)\sigma(\epsilon+\omega) \rangle$. Its calculation requires the average of a product of two expressions like Eq. (D2). Here we use the RMT relation

$$N^2 \langle \varphi_\alpha(j)\varphi_\alpha(k)\varphi_\beta(i)\varphi_\beta(l) \rangle = \delta_{\alpha\beta}[\delta_{ji}\delta_{kl} + \delta_{jl}\delta_{ki}] + \delta_{jk}\delta_{il}.$$

The three terms on the right hand side of the above equation correspond to the various paring possibilities of orbits as shown in Fig. 2. In particular, the first and second terms correspond to Figs. 2(a) and 2(b), while the third term corresponds to Figs. 2(c) and 2(d). Performing the sum over i, j, k, and l, the contribution of the first two terms is $I_{ab}(\omega) = 2\langle \Sigma_\alpha \delta_{\gamma/2}(\epsilon - \epsilon_\alpha)\delta_{\gamma/2}(\epsilon + \omega - \epsilon_\alpha) \rangle$, while the contribution of the third term is given by the correlator $I_{cd}(\omega) = \langle \Sigma_{\alpha\beta} \delta_{\gamma/2}(\epsilon - \epsilon_\alpha)\delta_{\gamma/2}(\epsilon + \omega - \epsilon_\beta) \rangle - 1/\Delta^2$. Thus

$$I_{ab}(\omega) = \frac{2}{\Delta}\int d\epsilon\, \delta_{\gamma/2}(\epsilon)\delta_{\gamma/2}(\epsilon+\omega) = \frac{2}{\Delta\pi}\frac{\gamma}{\omega^2+\gamma^2}$$

and

$$I_{cd}(\omega) = \int d\epsilon d\epsilon'\, \delta_{\gamma/2}(\epsilon)\delta_{\gamma/2}(\epsilon'-\omega)R(\epsilon-\epsilon'),$$

where $R(\epsilon - \epsilon')$ is the two-point function for the density of states of the GOE ensemble. Substituting the approximation $R(\epsilon-\epsilon') \simeq \mathrm{Re}\int dt t e^{i(\epsilon-\epsilon')t}/\pi^2$, and performing the integrals over ϵ and ϵ', we immediately obtain

$$I_{cd}(\omega) = \frac{1}{\pi^2}\mathrm{Re}\int_0^\infty dt\, t e^{-\gamma t + i\omega t} = \frac{1}{\pi^2}\frac{\gamma^2-\omega^2}{(\gamma^2+\omega^2)^2}.$$

Collecting these results we arrive at

$$Z^{(0)}(\omega) = \Delta^2(I_{ab}(\omega) + I_{cd}(\omega)) = \frac{2\Delta}{\pi}\frac{\gamma}{\omega^2+\gamma^2} + \frac{\Delta^2}{\pi^2}\frac{\gamma^2-\omega^2}{(\gamma^2+\omega^2)^2}.$$

Formula (59), apart from the prefactor ξ, is obtained by rescaling the variables in the above equation as $\Gamma = \gamma/\Delta$ and $\Omega = \omega/\Delta$.

We show, now, that in systems with a separation of time scales $\gamma_1 \gg \gamma_0$, the constant ξ in Eq. (59) is approximately unity. The separation of time scales implies that for times shorter than $1/\gamma_0$ the dynamics of the system may be approximated by that of a close chaotic system whose Hamiltonian will be denoted by $\mathcal{H}_0(\mathbf{x})$. In this case the first eigenfunctions of the classical propagator are constant functions corresponding to the ergodic distribution on the energy shell, namely, $\chi^l(\mathbf{x}) = \chi^r(\mathbf{x}) = [\int d\mathbf{x}\delta(\epsilon - \mathcal{H}_0(\mathbf{x})]^{-1/2}$. Substituting these eigenfunctions into expressions (57) and (58) for a and b, and evaluating $\xi = a^2/\langle\langle \rho_\phi \rangle\rangle^2/b$, one obtains $\xi = 1$.

[1] R. Schinke, *Photodissociation Dynamics* (Cambridge University Press, Cambridge, England, 1993).
[2] T. Ericsson, Phys. Rev. Lett. **5**, 430 (1960); Ann. Phys. (N.Y.) **23**, 390 (1963).
[3] R. T. Pack, E. A.Butcher, and G. A. Parker, J. Chem. Phys. **99**, 9310 (1993).
[4] D. Zhang and J. Z. H. Zhang, J. Chem. Phys. **101**, 3671 (1994).
[5] A. J. Dobbyn, M. Stumpf, H.-M. Keller, and W. L. Hase, J. Chem. Phys. **102**, 8 (1995).
[6] C. E. Porter, *Statistical Theory of Spectra: Fluctuations* (Academic Press, New York, 1965).
[7] T. A. Brody, J. Flores, J. B. French, P. A. Mello, A. Pandey, and S. S. M. Wong, Rev. Mod. Phys. **53**, 385 (1981).
[8] J. J. M. Verbaarschot, H. A. Weidenmüller, and M. R. Zirenbauer, Phys. Rep. **129**, 367 (1985).
[9] P. A. Mello, P. Pereyra, and T. H. Seligman, Ann. Phys. (N.Y.) **161**, 254 (1985).
[10] U. Smilansky, in *Chaos and Quantum Physics*, edited by M.-J. Giannoni, A. Voros, and J. Zinn-Justin (Elsevier, New York, 1990).
[11] C. H. Lewenkopf and H. A. Weidenmüller, Ann. Phys. (N.Y.) **212**, 53 (1991).
[12] Y. V. Fyodorov and H.-J. Sommers, J. Math. Phys. **38**, 1918 (1997).
[13] A. A. Abrikosov, L. P. Gor'kov, and I. E. Dzyaloshinski, *Methods of Quantum Field Theory in Statistical Physics* (Dover, New York, 1975).
[14] I. L. Aleiner and A. I. Larkin, Chaos, Solitons and Fractals **8**, 1179 (1997).
[15] O. Agam, B. L. Altshuler, and A. V. Andreev, Phys. Rev. Lett. **75**, 4389 (1995).
[16] For a review, see B. L. Altshuler and B. D. Simons, in *Proceedings of Les Houches Summer School, Session LXI, Mesoscopic Quantum Physics*, edited by E. Akkermans, G. Montambaux, J.-L. Pichard, and J. Zinn-Justin (North-Holland, Amsterdam, 1995).
[17] D. Ruelle, Phys. Rev. Lett. **56**, 405 (1986); J. Stat. Phys. **44**, 281 (1986).
[18] M. Pollicot, Ann. Math. **131**, 331 (1990).
[19] D. J. Thouless, Phys. Rep. **13**, 93 (1974).
[20] M. L. Mehta, *Random Matrices* (Academic Press, New York, 1991).
[21] Y. V. Fyodorov and Y. Alhassid, Phys. Rev. A **58**, R3375 (1998).
[22] Y. Alhassid and Y. V. Fyodorov, J. Phys. Chem. **102**, 9577 (1998).
[23] W. Lu, M. Rose, K. Pance, and S. Sridhar, Phys. Rev. Lett. **82**, 5233 (1999).
[24] M. V. Berry and K. E. Mount, Rep. Prog. Phys. **35**, 315 (1972).
[25] M. C. Gutzwiller, *Chaos in Classical and Quantum Mechanics* (Springer, New York, 1990).
[26] M. V. Berry, Proc. R. Soc. London, Ser. A **423**, 219 (1989).
[27] M. V. Berry, Proc. R. Soc. London, Ser. A **400**, 229 (1985).
[28] O. Agam, Phys. Rev. B **54**, 2607 (1996); and in *Supersymmetry and Trace Formulae: Chaos and Disorder* (Plenum, New York, 1999), pp. 133–151.
[29] M. V. Berry, Philos. Trans. R. Soc. London, Ser. A **287**, 237 (1977).
[30] The connected part of the correlator of two random variables, say g and f, is defined as $\langle gf\rangle_c=\langle gf\rangle-\langle g\rangle\langle f\rangle$.
[31] P. Cvitanović, Phys. Rev. Lett. **61**, 2729 (1988).
[32] P. Gaspard and S. A. Rice, J. Chem. Phys. **90**, 2225 (1989); **90**, 2242 (1989); **90**, 2255 (1991); **91**, 3279(E) (1989).
[33] P. Gaspard and D. A. Ramirez, Phys. Rev. A **45**, 8383 (1992).
[34] R. Blümel and U. Smilansky, Phys. Rev. Lett. **60**, 477 (1988); Physica D **36**, 111 (1989).
[35] R. A. Jalabert, H. H. Baranger, and A. D. Stone, Phys. Rev. Lett. **65**, 2442 (1990).
[36] Y.-C. Lai, R. Blümel, E. Ott, and C. Grebogi, Phys. Rev. Lett. **68**, 3491 (1992).
[37] E. Doron, U. Smilansky, and A. Frenkel, Phys. Rev. Lett. **65**, 3072 (1990).
[38] The Ruelle resonances of the four-disk system have been calculated by Gaspard and Ramirez [33] using the cycle expansion. In this calculation, the ratio of the distance between the disks to their radius is 3, while in the experiment [23] it is 4. Nevertheless, these theoretical calculations show that indeed the subleading Ruelle resonance are complex.
[39] K. B. Efetov, Adv. Phys. **32**, 53 (1983).